



HAL
open science

Lipid recovery from *Nannochloropsis gaditana* using the wet pathway: Investigation of the operating parameters of bead milling and centrifugal extraction

Vladimir Heredia, Jeremy Pruvost, Olivier Gonçalves, Delphine Drouin, Luc Marchal

► To cite this version:

Vladimir Heredia, Jeremy Pruvost, Olivier Gonçalves, Delphine Drouin, Luc Marchal. Lipid recovery from *Nannochloropsis gaditana* using the wet pathway: Investigation of the operating parameters of bead milling and centrifugal extraction. *Algal Research - Biomass, Biofuels and Bioproducts*, 2021, 56, pp.102318. 10.1016/j.algal.2021.102318 . hal-03246073

HAL Id: hal-03246073

<https://hal.inrae.fr/hal-03246073>

Submitted on 24 May 2023

HAL is a multi-disciplinary open access archive for the deposit and dissemination of scientific research documents, whether they are published or not. The documents may come from teaching and research institutions in France or abroad, or from public or private research centers.

L'archive ouverte pluridisciplinaire **HAL**, est destinée au dépôt et à la diffusion de documents scientifiques de niveau recherche, publiés ou non, émanant des établissements d'enseignement et de recherche français ou étrangers, des laboratoires publics ou privés.



Distributed under a Creative Commons Attribution - NonCommercial 4.0 International License

Lipid recovery from *Nannochloropsis gaditana* using the wet pathway: investigation of the operating parameters of bead milling and centrifugal extraction

Vladimir Heredia^a, Jeremy Pruvost^a, Olivier Gonçalves^a, Delphine Drouin^a, Luc Marchal^{a,*}

^a *Université de Nantes, Oniris, GEPEA, UMR 6144 F-44600, Saint-Nazaire, France*

Abstract

The aim of this work is to track and optimize lipid recovery from *Nannochloropsis gaditana* in wet extraction operations. **No significant differences in biomass concentration were found when disrupting microalgal suspensions of up to 30 g/L dry weight, but disruption efficiency differed depending on their physiological states.** It took 5.8 minutes in a bead milling device to disrupt 80% of the cells in a nitrogen-depleted culture (10-30 g/L), compared to 4.8 minutes for a nitrogen-replete culture (10-30 g/L). The **fatty acids** released were then recovered by two different methods: one using a centrifugal partition extractor device and the other using a continuous centrifugal extractor device. For the latter, Box-Behnken RSM analysis showed that the interaction between biomass concentration and solvent inlet rate had the greatest influence on lipid recovery. Up to 84% of the triacylglycerol was recovered using 7.9 g/L of algal suspension at 5.4 mL/min, and treated with 8.9 mL/min of 2-methyl-tetra-hydrofuran.

Keywords: Biodiesel, wet extraction, bead milling, centrifugal extraction, experimental design

1. Introduction

Over the last 20 years or so, biofuels from microalgae, such as biodiesel, have been considered as renewable fuels with which to address the energy crisis, and an option **with**

*Corresponding author

Email address: luc.marchal@univ-nantes.fr (Luc Marchal)

Preprint submitted to *Algal Research*

April 8, 2021

4 regard to mitigating climate change (CO₂ capture)[1]. The biodiesel production process
5 involves the production of fatty acids (FAs) by microalgae (which are stored under stress
6 conditions), the recovery of these energy-rich compounds, and further chemical conversion
7 of them.

8 There are several microalgae species which can accumulate FAs. The *Nannochloropsis*
9 genus, in particular, is a diverse collection of microalgae comprising 6 species and several
10 sub-strains; most of these have been widely studied for biodiesel production due to their
11 high lipid content under conditions of stress (up to 60%_X) [2, 3, 4, 5]. *Nannochloropsis*
12 *gaditana* is one of the most promising strains, producing high levels of lipids [6]. It is
13 well known that applying stresses such as nitrogen limitation and high light exposure
14 to microalgae triggers the accumulation of FAs, in particular Triacylglycerol molecules
15 (TAG) [6, 7, 8]. Stress also seems to affect cell resistance to disruption. It has been
16 shown that the *Nannochloropsis* genus has a relatively thin cell wall in optimal growing
17 conditions, but when it is exposed to nitrogen limitation the mechanical resistance of the
18 cell is somehow increased [2, 9]. This effect could be linked to changes in the cell size or
19 lipid fraction of the cell wall [10, 11, 12].

20 Although many technologies have been developed for FAs recovery [13, 14, 1, 15, 16],
21 not all of them can be applied in the biodiesel context, mainly because the processes
22 used are not always as sustainable, energy-efficient or economically viable as expected.

23 Compared to the energy-intensive operations of the dry pathway, such as biomass
24 drying and solid-liquid extraction, the wet pathway with its technique of cell disruption
25 combined with liquid-liquid extraction is a tested option for developing an energy-efficient
26 process for recovering lipids from microalgae [9, 17, 18, 19, 20]. During cell disruption,
27 many intracellular components, including FAs, are released into the liquid culture and
28 can then be recovered using solvents. This dispenses with the drying or dewatering step
29 involved with the dry pathway and reduces the overall energy required [17, 21, 22, 23].

30 Cell disruption techniques include biochemical methods (*e.g.* enzymes, chemical
31 treatments, osmotic shock) and mechanical methods (*e.g.* microwaves, ultrasonication,
32 bead milling, high-pressure homogenization, electroporation) [24, 16]. Mechanical meth-
33 ods are advantageous because additional reactive compounds, which may degrade or
34 degenerate beneficial intracellular compounds, are not required. Also, mechanical meth-

35 ods may be less species-specific than biochemical methods, and for some a wider range
36 of wet biomass concentrations can be treated even for continuous operation. However,
37 these techniques still need improvement in terms of energy consumption and biomass
38 concentration efficiency before they can be used in the wet pathway process for biodiesel,
39 and in terms of understanding and optimizing the undesired effects of some microalgal
40 intracellular compounds on other downstream processes (*e.g.* liquid-liquid extraction by
41 solvents)[24, 9, 25, 26, 16, 23].

42 Traditional lipid extraction methods by solvents use a mixture of CHCl_3 and methanol
43 [27, 28]. Although non-protic or aprotic polar solvents like hexane and CHCl_3 [29] have
44 high lipid-extraction yields, their use at industrial scale would exacerbate environmen-
45 tal and health problems [30]. Aprotic solvents like ethyl acetate and 2-methyl-tetra-
46 hydrofuran are an alternative; these are also known as green solvents because they are
47 produced from renewable raw materials. 2-methyl-tetra-hydrofuran, heptane and 8 oth-
48 ers have been screened previously for their efficiency in short-time wet extraction. 2-
49 methyl-tetra-hydrofuran in particular minimizes the energy needed for solvent recycling
50 and presents low solubility in water [9].

51 Liquid-liquid (L-L) extraction is a method widely used for separating a solute from one
52 liquid (*i.e.* microalgal culture feed) into another with a relative preference for the solute
53 (*i.e.* solvent). Efficiency depends mainly on the distribution coefficient of the L-L sys-
54 tem (and therefore the choice of solvent), the surface and time of contact between phases
55 (related to mixing), the concentration of the solute (*i.e.* lipid availability) and operat-
56 ing parameters such as temperature and rate of solvent/feed. At industrial scale, these
57 parameters can be modulated in mixers/reactors (batch operation) or mixer-settlers and
58 columns (continuous operation). However, this equipment often requires an additional
59 separation operation (large separatory funnel or industrial centrifugation/decantation).
60 In this regard, an approach employing intensified operations would integrate these tech-
61 nologies and eventually lead to smaller, more energy-efficient process equipment [31, 32].

62 One way of intensifying wet extraction is to use processes based on centrifugal force,
63 for improved mixing and separation. Systems like continuous centrifugal extraction
64 (CCE) (Fig. 1a) are designed for continuous L-L extraction and simultaneous sepa-
65 ration of the phases [33]. CCE mixes two input streams - solvent and algal culture feed

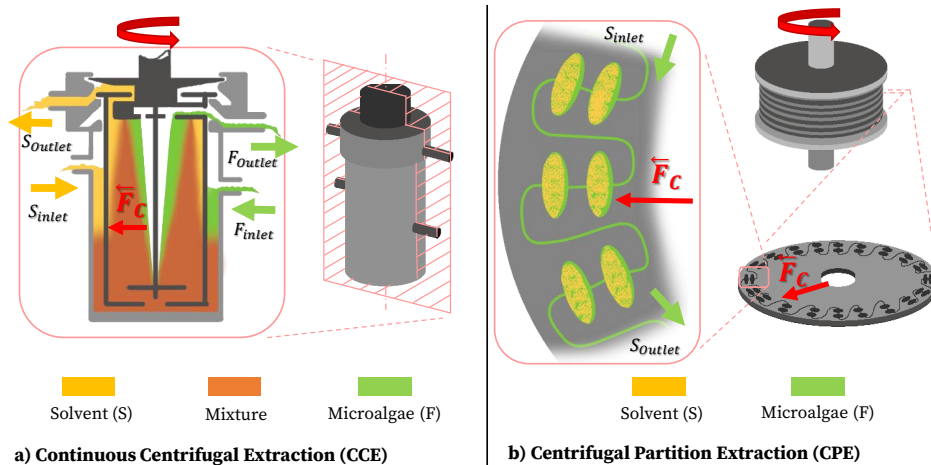


Figure 1: Continuous Centrifugal Extraction and Centrifugal Partition Extraction comparison diagrams. F_C is the centrifugal force vector.

66 (rich in lipids) - in a common rotary chamber, the speed of which can be modulated.
 67 Under the right conditions, two separate outlet flows are recovered during extraction: the
 68 raffinate fraction - which is mostly lean culture, and the extract fraction, which is mostly
 69 solvent. This equipment is promising for reducing solvent consumption and simplifying
 70 scale-up of the wet-extraction process due to its adjustable flow-rate capacity and the
 71 ability to connect several modules in series. However, there are no reports on the use of
 72 CCE for purely biotechnological applications or biofuel production [34, 32].

73 Another interesting approach for wet-extraction is to use a centrifugal partition ex-
 74 traction (CPE) device (Fig. 1b). These devices have been widely used for separation
 75 and recovery purposes in the biotechnology and nutrition industries [33]. The principle
 76 is similar to L-L chromatography but with no solid support to retain the solutes; it is
 77 based on the partition coefficient between two non-miscible solvents. CPE devices such
 78 as, centrifugal partition chromatography (CPC) have a series of small chambers filled
 79 with solvent as a stationary phase. The stationary phase inside is maintained by apply-
 80 ing a centrifugal force to the entire series of chambers. A mobile phase is then pumped
 81 into the system, enabling interaction with the solvent. This way, the solvent elutes the
 82 solutes every time it enters the chambers. With this technology, the amount of solvent
 83 used and the operating time are considerably reduced compared to conventional extrac-

84 tion processes, including CCE [35]. For this reason, CPE is a useful comparison point
85 for efficiency.

86 Some parameters still need to be adjusted for scaling up centrifugal lipid extraction
87 for biodiesel production. These include: 1) the availability of lipids for the extraction
88 (lipid concentration function and percentage of disrupted biomass); 2) the establishment
89 of an adequate solvent/feed ratio for optimal mass transfer; 3) the absence of emulsion
90 (regularly promoted by the release of intracellular proteins and pH changes after cell
91 disruption).

92 Analyzing the role of the above parameters in isolation in the extraction process would
93 be inefficient in terms of time, resources and unknown related interactions. One strategy
94 for analyzing and optimizing the multiple factors that interact in the phenomenon is
95 the response surface methodology (RSM). However, prior to running an RSM, a few
96 exploratory experiments are required to ascertain the trends of the variables.

97 The aim of this work is therefore to enhance lipid recovery from *Nannochloropsis*
98 *gaditana* by first maximizing lipid availability via bead milling, then optimizing the
99 main parameters using CCE technology. The optimal lipid recovery obtained is then
100 compared with a reference CPE and the resulting operational problems discussed in
101 terms of biodiesel application.

102 2. Materials and Methods

103 2.1. Microalgal Cultures

104 The microalga *Nannochloropsis gaditana* CCMP527 (NCMA, USA) was grown in
105 artificial sea water (ASW) [36] enriched with CONWAY solution as the culture medium.
106 ASW is prepared using (mM): NaCl, 248; Na₂SO₄, 17.1; KCl, 5.49; H₃BO₃, 0.259;
107 NaF, 0.045; MgCl₂-6H₂O, 32.24; CaCl₂-2H₂O, 0.626; KBr, 0.497; SrCl₂-6H₂O, 0.056;
108 NaHCO₃, 1.42. CONWAY solution uses NaNO₃ as the source of nitrogen, at 10.6 mM.
109 However, for the experiments referred to as N-replete (optimal conditions), the amount of
110 NO₃ was doubled to 21.2 mM to ensure there was no nitrogen limitation. For the cultures
111 referred to as N-depleted (starved conditions), a CONWAY solution was prepared without
112 NO₃, and this was added in the same quantity as for the replete culture. All cultures

113 were inoculated with a 10% inoculum/medium ratio using a pre-culture in exponential
114 cell growth.

115 Three photobioreactors (PBRs) were used to supply enough biomass for the work. For
116 the early experiments related to cell disruption optimization and solvent choice, two were
117 set outdoors in France in late summer 2018 (47°15'06.5" N, 2°15'34.5" W) in 170-litre
118 flat-panel airlift PBRs (Subitec, Germany). These reactors were operated in batch mode
119 with the pH regulated at 8 by manual injection of 98% CO₂ (gas). For the experiments
120 related to Box-Behnken RSM, a single 170-litre flat-panel airlift PBR (HECtor PBR)
121 was operated indoors in batch mode. A description of the reactor is given by Pruvost
122 et al. [37]. This reactor was irradiated with artificial LED light, simulating the average
123 annual irradiation (photon flux density 269 $\mu\text{mol}/\text{m}^2\cdot\text{s}$) and solar cycles of the above
124 outdoor conditions. The pH was also set at 8 by automatic CO₂ (gas) injection.

125 The biomass from the depleted and replete cultures was harvested using a continuous
126 centrifuge (DRA320VX Rousselet Robatel, France) at 6000 rpm (8064 rcf). The sludge
127 (biomass concentration 40 g/L) was then diluted using a phosphate buffer saline (PBS)
128 solution to obtain 1, 5, 10, 20 and 30 g/L for cell disruption optimization, and 2, 5 and
129 10 g/L for the RSM. Note that in addition to the biomass concentration usually obtained
130 directly from the culture system (1-5 g/L), the range of biomass concentrations in this
131 case was increased to 30 g/L to simulate the possible use of other pre-concentration
132 processes for potential medium recycling (such as dissolved air flotation).

133 2.2. Dry Weight Analysis

134 Glass fiber filters with a pore diameter of 0.45 μm (Whatman GF/F) were pre-
135 weighed. 10 mL samples were taken from the PBRs and filtered in triplicate. The
136 filtered biomass was then washed with 3 equal volumes of NH₄HCO₂ 1.19 M and 3 equal
137 volumes of MiliQ water to remove culture medium salts. The filters were dried at 103
138 °C for 1 hour (no further time needed to achieve weight stabilization) and then weighed.
139 The biomass concentration (represented by X) was considered as the weight difference
140 between the dry biomass and the empty filters for each culture volume. The values
141 reported correspond to the mean values in a triplicate dry weight assay.

142 *2.3. Bead Milling*

143 To carry out cell disruption, a continuous bead mill was used in the laboratory
144 (DYNO-Mill KD, Multilab, WAB, Switzerland). The grinding chamber (≈ 0.561 L)
145 connected to an agitator disc (64 mm diameter) was filled to 80% with 0.5 mm diameter
146 glass grinding beads. During the process, milling was carried out at an impeller tip speed
147 of 14 m/s and a flow biomass inlet rate of 9 L/h, with reference to Zinkoné et al. [25].

148 Three dilutions (10, 20, 30 g/L) for each N-depleted and N-replete outdoor culture
149 were passed through the bead milling device between 1 and 5 times. The corresponding
150 aliquot was analyzed after each time to determine the associated disruption rate.

151 *2.4. Quantification of Cell Disruption*

152 The cells were counted digitally using image analysis and a Malassez cell-counting
153 chamber under microscope. First, a diluted sample was prepared to avoid saturating the
154 number of cells per image, but enough to provide a representative aliquot of the culture
155 [25]. Then a Malassez double chamber was prepared and focused at 40x using an optical
156 microscope connected to a camera (Axio MRC Cam at Axio Scope A1 microscope, Carl
157 Zeiss, Germany). The camera took 40 pictures of each sample, which were then analyzed
158 using image-analysis software (ImageJ v.1.52o, NIH, USA) to distinguish images-like-
159 noise and images-like-cells. The cell surface was calculated in μm^2 for all images-like-cells,
160 based on the distance-to-pixel ratio.

161 This method identified the cell size, shape and surface distribution of the original
162 culture and compared it to the corresponding values after cell disruption enabling cell
163 debris to be distinguished from undisrupted cells. The cell count and statistical informa-
164 tion were then gathered using a MATLAB algorithm (Math-Works, US). Prior to using
165 this method, it was validated with direct microscope counting (data not shown).

166 The microalgal cell disruption rate τ_D was defined as the complementary fraction of
167 the ratio of cells counted after bead milling to those counted before the process.

168 *2.5. Total Fatty Acid (TFA) and Triacylglycerol (TAG) Extraction Efficiency and Quan-*
169 *tification*

170 To measure the TFA content, the organic fractions from extraction experiments were
171 recovered and the corresponding solvent evaporated. The following analysis protocol is

172 adapted from Moutel et al. [38]. An internal standard solution of a known C17:0 fatty
173 acid concentration and $\text{CHCl}_3/\text{MeOH}$ was added to corroborate the subsequent findings.

174 To summarize, the sample was derivatized using BF_3 (catalyst) and MeOH at 96°C
175 for 10 minutes (VWR International, US). Following the reaction, the sample was washed
176 using distilled water saturated in hexane to remove catalyst residues. The organic phase
177 was then recovered and measured by gas chromatography using a flame ionization de-
178 tector (GC-FID, Agilent Technologies, USA). Fatty acid methyl esters (FAMES) were
179 determined by comparing their retention time with those of the standards ones used for
180 calibration. The concentration of each FAME was calculated with Chemstation software
181 (Agilent Technologies, USA), using C17:0 fatty acid as the internal standard.

182 TAG content was determined by taking an aliquot of the organic fractions from the
183 extraction experiment and processing it by HPTLC (CAMAG, Switzerland). Samples
184 between 1 and 20 μL were placed on silica gel plates (20 x 10 cm; Merck Group, Germany)
185 by auto-sampler. A self-designed mix of polar and non-polar lipids (Sigma-Aldrich, US)
186 was also placed on the plate as the standard. After sample migration, the plate was
187 revealed in a chromatogram immersion device with a TLC plate heater, using an ortho-
188 phosphoric acid and copper sulphate solution. Data acquisition was by TLC Scanner 3
189 (VisionCats, CAMAG, Switzerland) and related software.

The results for TFA or TAG per gram of algal biomass treated are shown as $\text{TFA}\%_X$
or $\text{TAG}\%_X$. The extraction efficiency is represented by:

$$\eta_{E,i} = (i_j)/(i_{\text{CHCl}_3/\text{MeOH}}) \quad (1)$$

190 where i is either $\text{TFA}\%_X$ or $\text{TAG}\%_X$ extraction carried out with a specific solvent, j .

191 2.6. Choice of Solvent and Standard Extractions

192 To find out either the TFA or TAG content, $\text{CHCl}_3/\text{Methanol}$ 2:1 v/v (Fisher Sci,
193 US) was used as a reference solvent for extractions. Other solvents used for comparison
194 assays were heptane, Hep (Emsure-Merck, Germany), ethyl acetate, EtoAc (Fisher Sci,
195 US) and 2-methyl-tetra-hydrofuran, Me-THF (Acros Organics-Thermo Fisher Sci, US).
196 Their main properties are summarized in Table 1.

197 Samples from the depleted cultures were passed through a high-pressure homogenizer
198 (Constant Systems Ltd, UK) three times at 2.7 Kbar and 10°C . Passing the samples

Table 1: Main physicochemical properties of heptane (Hep), ethyl acetate (EtoAc) and 2-methyl-tetrahydrofuran (Me-THF)

	Hep	EtoAc	Me-THF
<i>Molecular Formula</i>	C ₇ H ₁₆	C ₄ H ₈ O ₂	C ₅ H ₁₀ O
<i>Density at 20° C - ρ_S (g/mL)</i>	0.684	0.902	0.854
<i>Vapor pressure at 20° C (mmHg)</i>	34.5	73	102
<i>Boiling temperature at P_{atm} (° C)</i>	98.4	77.1	80.2
<i>Viscosity at 25° C (cP)</i>	0.376	0.423	0.46
<i>Solubility in water at 20° C (wt%)</i>	2.2 (25° C)	8.7	14.1
<i>Reference</i>	[39]	[39]	[40]

199 through the equipment three times ensured total destruction of the cells, which was
 200 verified by microscope observation. The suspension was mixed with the respective solvent
 201 at 1:2 v/v (solvent per aqueous phase) for 4 hours at 23 °C, the organic phase was then
 202 recovered and the TFA and TAG concentration determined for the solvents tested.

203 2.7. Continuous Centrifugal Extraction

204 The extraction system used was a mono-stage continuous centrifugal extraction (CCE)
 205 device - type BXP 012 (Rousselet Robatel, France) using N-depleted biomass from the
 206 HECtor PBR. Biomass concentration was adjusted to the target values (2,5,10 g/L) and
 207 then disrupted in the bead mill to obtain a cell disruption rate τ_D of more than 90%
 208 (verified by microscope observation). This suspension was considered as the inlet feed.

209 The rotation speed of the CCE device was set beforehand at between 2000 and 4000
 210 rpm (107-430 rcf) depending on the experiment run. After approximately 20 seconds, the
 211 speed was stable and the solvent and feed inlet rates (S and F) were set at the established
 212 flow rate into the system. After an additional 30 - 60 seconds, the extract and raffinate
 213 fractions (E and R) began to flow out normally and were recovered at the same inlet flow
 214 rate, which also enabled verification of the total flow supplied ($ToT = S + F = E + R$).
 215 Around 30 mL from each outlet current (E and R) was then collected and analyzed
 216 identically by GC-FID and HPTLC to obtain the TFA/TAG extraction efficiency $\eta_{E,i}$
 217 for the experiment run.

218 *2.8. Experimental Design for Continuous Centrifugal Extraction*

219 A Box-Benhken experiment was designed using the data collected from the bead
220 milling optimization and the more efficient solvent. The CCE variables chosen for Box-
221 Benhken RSM optimization were biomass concentration (after harvesting), solvent inlet
222 rate and feed inlet rate. For detailed information on the design of the Box-Benhken and
223 related data processing, see Appendix A.

224 All the experiment runs were immediately batched-executed at 25°C within the first
225 30 minutes of bead milling, to avoid undesirable reactions due to interaction between the
226 medium ions and the cell cytoplasm. Samples from each observation unit were stored at
227 -80°C for determination of further TFA/TAG extraction efficiency ($\eta_{E,i}$).

228 Where emulsification was unavoidable, samples were still taken but centrifuged at
229 6000 rpm (4226 rcf) and 4°C for 10 minutes (Hettich, Germany), to separate the phases
230 from the two outlets. The organic phase was then analyzed by the same methods as
231 described above.

Using the data obtained according to the experimental design, the specific solvent
consumption Γ_j was calculated as follows:

$$\Gamma_j = (S \cdot \rho_j) / (F \cdot X \cdot \eta_{E,i}) \quad (2)$$

232 where S is the solvent inlet rate and F the feed inlet rate (both in mL/min); ρ_j is the
233 solvent density in g/mL, X is the biomass concentration in the feed in g/mL and $\eta_{E,i}$ is
234 the extraction efficiency. In this work, Γ_j was only calculated for the optimized condition
235 in the CCE and analysis of the comparison with the CPE.

236 *2.9. Centrifugal Partition Extraction*

237 Centrifugal partition extraction (CPE) was carried out for comparison with the final
238 CCE optimization value. Two liters of N-depleted culture at 5 g/L biomass concentration
239 X were passed through the bead mill several times to obtain a cell disruption rate τ_D of
240 more than 90% (verified by microscope observation). This suspension was treated with
241 CPE.

242 The CPE device (Model A, Kromaton, France) was fitted with a short column (231
243 chambers) to carry out TAG extraction with Me-THF. The equipment was set for 1 stage

Table 2: Culture conditions after batch operations. X is biomass concentration, TFA total fatty acid content and TAG triacylglycerol content.

Culture system		X (g/L)	SE (n = 3)	TFA content (% _X)	TAG content (% _X)	Index 480/662 nm
Outdoor	N-Replete	2.29	2.29	8.7	2.2	0.51
Outdoor	N-Depleted	0.54	0.02	28.1	13.4	1.83
Indoor	N-Depleted	1.52	0.01	32.2	28.6	3.34

244 at 900 rpm (59 rcf, [41]) in non-continuous mode for a column volume of 270 mL and
 245 a solvent volume of 140 mL. The disrupted culture suspension was then passed through
 246 the system at 25 mL/min, allowing 5 minutes for the extraction (residence time). The
 247 solvent and feed volumes and rates were based on Marchal et al. [42] and Ungureanu
 248 et al. [35]. The extracted fraction was recovered and analyzed for TAG content and
 249 consequently TAG extraction efficiency ($\eta_{E,TAG}$).

250 3. Results and Discussion

251 3.1. Final Culture Conditions

252 Table 2 shows a summary of the final conditions of the cultures used to produce the
 253 biomass. After 11 days, the final biomass concentrations for N-depleted and N-replete
 254 outdoor cultures were 0.54 and 2.29 g/L (SE = 0.02 and 2.29; n = 3) respectively,
 255 with 28.1%_X and 8.7%_X of TFA and 13.4%_X and 2.2%_X of TAG respectively. The
 256 absorbance 480/662 nm index was measured [43] as a reference to compare stress levels
 257 between the PBRs. The N-depleted and N-replete values on the final day were 1.83
 258 and 0.51 respectively, indicating that the carotenoids-to-chlorophyll ratio had a strong
 259 influence on the N-depleted culture and confirming cell stress compared to the N-replete
 260 culture, as expected.

261 The indoor PBR culture was ended after 13 days. The final biomass concentration
 262 was 1.52 g/L (SE = 0.01; n = 3) with 32.2%_X TFA and 28.6%_X TAG. The 480/662 nm
 263 index was 3.34 at the end of the culture, which also corroborates the cell stress.

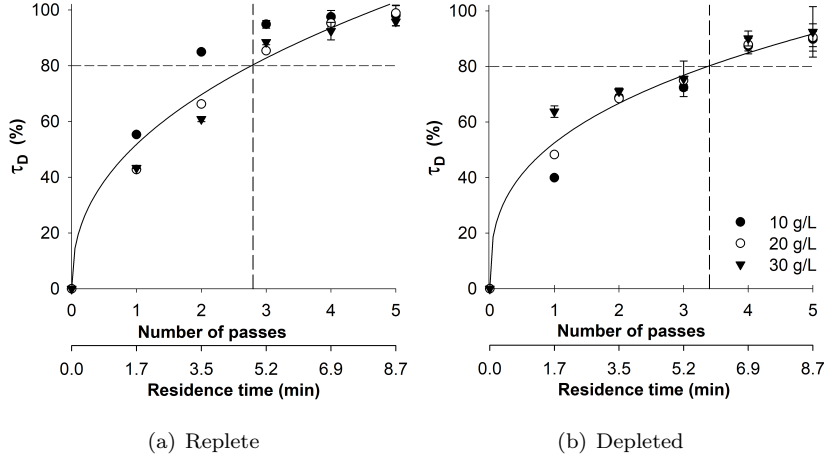


Figure 2: Disruption kinetics at bead milling for N-replete and N-depleted cultures. The disruption rate τ_D is plotted for each biomass concentration condition X , and the two-parameter power regression for each physiological state. Error bars for CI ($n \approx 20$, $\alpha = 0.05$)

264 3.2. Cell Disruption Optimization

265 Fig. 2 plots the cell disruption rate as a function of the physiological state (as a conse-
 266 quence of cells adapting to the culture medium) and biomass concentration, throughout
 267 the operating period. Three different biomass concentrations from two different medium
 268 conditions (replete and depleted) were processed in a bead mill to find the residence time
 269 required (*i.e.* number of passes) to achieve a cell disruption rate of 80%. A one-way anal-
 270 ysis of the variance applied to the disruption rate results from the biomass concentration
 271 groups at each physiological state revealed that there were no statistically-significant
 272 differences between the groups (replete: $F(2, 12) = 0.31$, $p = 0.74$; depleted: $F(2, 12)$
 273 $= 0.22$, $p = 0.81$). Based on this consideration, the whole data set for each physiological
 274 state was arranged in a two-parameter power regression, as shown in Fig. 2 ($R^2 = 0.9619$
 275 for replete, $R^2 = 0.9776$ for depleted), and the regression equation enabled calculation
 276 of the exact residence time needed for bead milling to disrupt 80% of the cells: 4.8 min-
 277 utes for replete culture and 5.8 minutes for depleted culture (both for concentrations of
 278 between 10 and 30 g/L). The difference is more evident in Fig. 2 where $\tau_D > 80\%$. A
 279 minimum of three passes are required for the replete culture (Fig. 2a) and four passes
 280 for the depleted culture (Fig. 2b). A comparison of the τ_D from different physiological

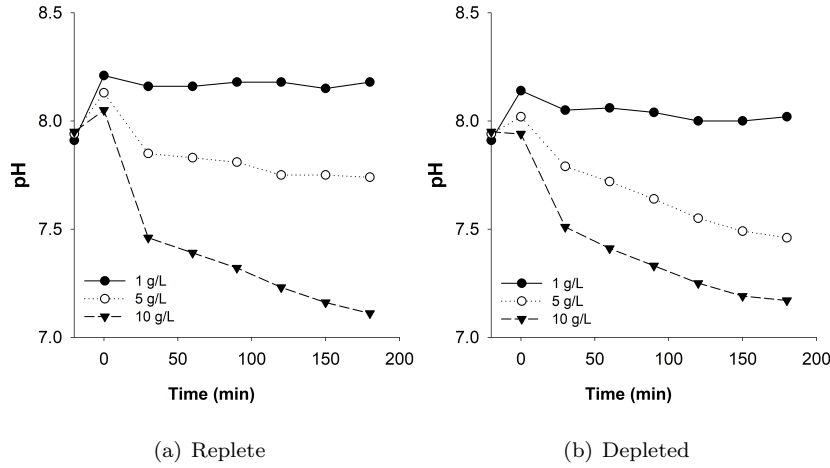


Figure 3: pH value of microalga suspension after passing 4 times through a bead mill for N-replete (a) and N-depleted (b) cultures. For each graph, the value on the left represents the pH before milling; the value at zero represents the moment immediately after milling ($n = 1$).

281 states shows that *N. gaditana* presents more mechanical resistance to milling when it
 282 is harvested in nitrogen-depleted conditions. A similar result using *Nannochloropsis sp.*
 283 was obtained by Angles et al. [9].

284 The final pH value after bead milling is important to preserve the integrity of the
 285 molecules to be recovered, and also the workability of the suspension for further steps,
 286 mainly emulsification of the lipids and proteins released during the process. For this
 287 reason, the pH was monitored for biomass concentrations 1, 5 and 10 g/L and for the
 288 two physiological conditions, after cell destruction. The initial pH was 7.9 for each, as
 289 shown in Fig. 3. The 10 g/L suspensions for both physiological conditions stabilized
 290 the pH almost immediately after disruption (8.2 for replete and 8.0 for depleted). In
 291 addition, the 5 g/L suspension of the N-replete culture had a stable and lower pH of 7.8
 292 after 120 minutes. The N-depleted condition at the same concentration and in the same
 293 period did not achieve stability (around pH 7.5). The same was observed for the highest
 294 suspension concentrations (10 g/L) for both physiological conditions in the 180 minutes
 295 test. These conditions tended to attain even lower pH values (around pH 7). This could
 296 be explained by the fact that when 5 and 10 g/L cultures are milled, ions like H^+ and
 297 other organic compounds are released in proportion to cell concentration and stress level

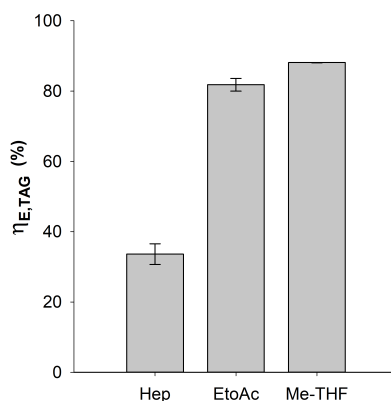


Figure 4: Triacylglycerol extraction efficiency for heptane (Hep), ethyl acetate (EtoAc) and 2-methyl-tetra-hydrofuran (Me-THF). Error bars for SE ($n = 2$)

298 (these compounds possibly being accumulated under stress conditions as a cell regulation
 299 mechanism [44]). Presumably, the release of these ions and molecules, added to the rest
 300 of the culture medium, could interact until the whole solution reaches an equilibrium.
 301 The pH stabilization time would depend on the abundance of these molecules and their
 302 interaction in the final mixture. It would therefore appear that the suspension needs to
 303 be processed for the first 50 minutes after cell disruption, at most, to avoid any undesired
 304 interaction, which could affect the recovery process.

305 3.3. Choice of Solvent for Extraction

306 Fig. 4 shows the extraction efficiency results for N-depleted biomass using the three
 307 solvents tested. Me-THF and EtoAc showed a similar extraction efficiency $\eta_{E,TAG}$: up to
 308 88% and 82% respectively. Heptane had the lowest at 34%. In all cases, TAG represented
 309 89% of the measured TFA, showing that the solvents used have no relevant selectivity
 310 for TAG.

311 In addition, by using cell destruction prior to extraction, the solvents (or mixtures)
 312 did not depend on their ability to draw lipids from the cell (such as 2:1 v/v $\text{CHCl}_3/\text{MeOH}$
 313 [28]) but only on their affinity with lipid molecules, since TAG molecules were already re-
 314 leased into the medium. This enabled maximization of extraction efficiency and thereby
 315 reduction of the amount of solvent used, which would also significantly reduce the in-
 316 vestment in solvent required for the whole wet extraction process.

317 As a result, Me-THF will be selected for future experiments as the best of the three
318 solvents for recovering TAG.

319 *3.4. Centrifugal Partition Extraction*

320 Centrifugal partition extraction (CPE) was used only as a reference to compare the
321 specific solvent consumption (Γ_{Me-THF}) of the optimal CCE results from the Box-
322 Benhken RSM.

323 For a single TAG extraction carried out with a CPE device, it was possible to treat
324 2 L at a biomass concentration 5 g/L with only 140 mL of solvent.

325 These values represent a TAG extraction efficiency $\eta_{E,TAG}$ of 83% (SE = 3%, n = 3),
326 which corresponds to a specific solvent consumption of Γ_{Me-THF} of 27.7 g_{Me-THF}/g_{TAG}.

327 *3.5. Continuous Centrifugal Extraction*

328 The Box-Benhken RSM was chosen as the method for optimizing the main CCE
329 parameters. The optimal value obtained with this method, added to the bead milling
330 results, was expected to provide relevant information on the overall efficiency of the
331 wet-extraction method in the biodiesel context.

332 Pre-tests were run prior to the main analysis to clarify the operating CCE work zone.
333 Emulsions were readily obtained when the rotation speed of the CCE device exceeded
334 certain limits. These limits varied for each observation unit (OU) but were within the
335 5000 to 6000 rpm range (670 - 966 rcf). A relationship was observed between this rota-
336 tional speed limit and the total supplied flow (ToT) for the different substances. Higher
337 speeds promoted separation of the phases, but also the formation of emulsion. This phe-
338 nomenon could be due to Taylor vortexes occurring during the centrifugal extraction and
339 driving more complex variations in fluid dynamics when the rotation speed was increased
340 [45, 46]. There is therefore a compromise between emulsification and separation when
341 using a CCE module.

342 Another factor that could influence emulsification and therefore extraction efficiency
343 ($\eta_{E,i}$) is the release of intracellular material into the medium. It has been shown that
344 some microalgae proteins have emulsifying properties [47]. Similarly, the cell debris
345 could also form particle-stabilized emulsions known as Pickering emulsions [48]. Biomass
346 concentration and disruption rate, therefore, also influence this phenomenon; for a given

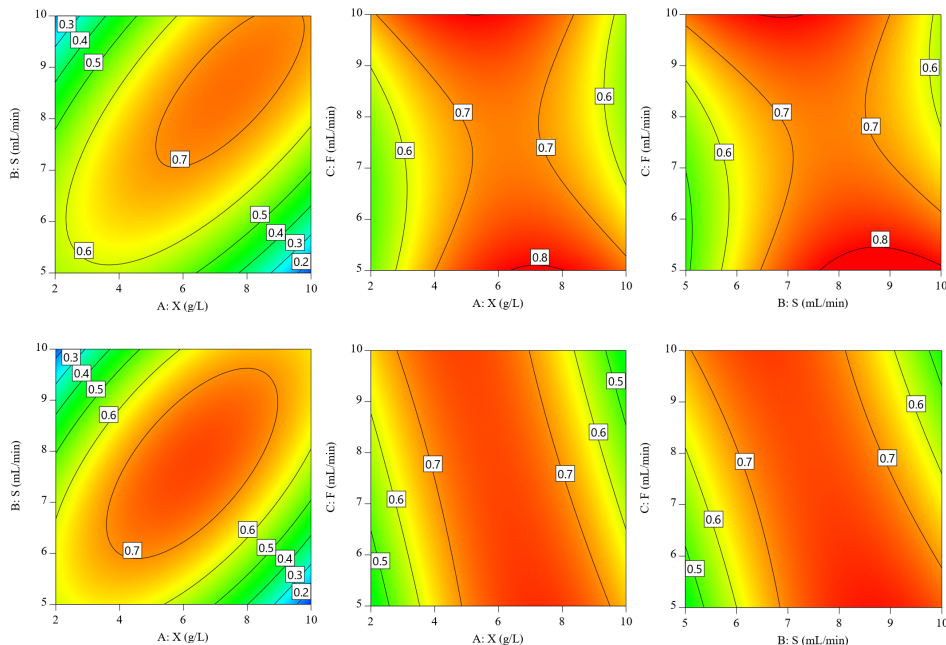


Figure 5: Contour graphs for each interaction between sources for the regression model obtained by Box-Behnken for extraction efficiency, $\eta_{E,i}$ response. The contour lines represent extraction efficiency, $\eta_{E,i}$ levels; a), b) and c) for **Total Fatty Acid (TFA)** and d), e) and f) for **Triacylglycerol (TAG)**.

347 high biomass suspension, increasing the disruption rate τ_D will also release emulsifying
 348 molecules/particles. Accordingly, additional pre-tests were run to clarify the biomass
 349 concentration range to avoid emulsification as far as possible. Normally, cultures above
 350 10 g/L are unmanageable for extraction due to the immediate appearance of an emulsion,
 351 even when working at low S/F ratios or low rotation speeds (< 4000 rpm / 429 rcf). For
 352 example, when working with suspensions above 10 g/L of biomass, emulsions appeared
 353 from 3500 rpm (329 rcf). A higher rotation speed was therefore required for recovering
 354 the same outlet flow rates (since $ToT = S + F = E + R$), although no solvent was
 355 recovered, just an enhanced emulsion. These pre-tests defined the operational range
 356 of biomass concentration as between 2-10 g/L for RSM analysis. Protein content and
 357 operational pH were not considered as variables for RSM.

358 The RSM experimental results are detailed in Appendix A, Table A.3. The resulting
 359 contour graphics (Fig. 5) describing the extraction efficiency as a response of the oper-

360 ational variables may therefore be useful for navigating within the limits of the CCE.
361 Using the biomass - solvent interaction ($X - S$), as a first reference, Figs. 5a and 5d show
362 the maximal extraction efficiency $\eta_{E,i}$ as being within S : 7-10 mL/min and X : 5-10 g/L.
363 This zone can therefore be transposed to the $X-F$ and $S-F$ interactions (Figs. 5b, 5c,
364 5e, 5f) where higher efficiencies are found at a low feed rate.

365 The numerical results obtained (see Appendix A) provide a tool for locating the
366 optimal point for the three simultaneous sources. It was found that $\eta_{E,TFA} = 0.93$ at X
367 = 8.3 g/L, $S = 9.2$ mL/min, $F = 5.0$ mL/min and $\eta_{E,TAG} = 0.84$ at $X = 7.9$ g/L, $S = 8.9$
368 mL/min and, $F = 5.4$ mL/min. Both efficiency points were consistent with the previous
369 analyses. The values obtained were higher than with the $CHCl_3$ /methanol wet extraction
370 (extraction efficiency, $\eta_{E,i} = 50\%$) carried out by Angles et al. [9]. Remember, however,
371 that the values correspond to the 80% of lipids released in the bead milling operation.

372 With the optimal point obtained by the experiment design, the specific solvent con-
373 sumption for CCE was determined as $\Gamma_{Me-THF} = 213.8$ g_{Me-THF}/g_{TAG}.

374 Note that Γ_{Me-THF} is linked to the energy consumption for the whole biodiesel
375 process, since more energy is required for distilling each gram of solvent used to produce
376 each liter of biodiesel. These values show that if scaled up, CPE technology could save 7.8
377 times more solvent than CCE, even though the two technologies have similar extraction
378 efficiencies.

379 However, the results for CCE could be improved. On the one hand, this work has
380 demonstrated the relationship between stress levels, biomass concentration and the re-
381 lease of intracellular material with the formation of emulsion, and has revealed the work
382 zone to be avoided when carrying out CCE. In this regard, more research on the optimiza-
383 tion of hydrodynamics in the CCE chamber could enable working with higher biomass
384 concentrations, which would increase recovery. On the other hand, CCE efficiency can
385 also be improved by using several devices connected in series (the present work relating
386 to a single module). This approach is also valuable in terms of the scalability of the
387 operation, which is one of the biggest advantages of CCE over CPE.

388 As stated, many factors other than those relating to the appearance of emulsification
389 (such as pH and temperature) that were not studied in detail in the present work, in-
390 teract during centrifugal extraction and should be investigated for future experiments in

391 biodiesel production.

392 The optimal wet extraction yield of 73% obtained with bead milling combined with
393 CCE (using Me-THF) has been demonstrated as a high-performance TAG recovery tech-
394 nique with the advantage of scalability for the biodiesel process. The process may perform
395 better than extraction yields in the literature. For example, different solvent mixtures
396 and cell disruptions for *N. gaditana* were tested by Ryckeboosch et al. [49], where solvents
397 such as hexane/isopropanol, ethyl acetate/hexane and ethanol were found to be the best
398 of six, with extraction yields of 58%, 46% and 52% respectively. Similarly, Sati et al.
399 [50] reviewed extraction yields from other pre-extraction treatments such as mechanical
400 (35%), surfactant (78%) and enzymatic lysis (73%). There are other techniques effective
401 for biodiesel application too, such as the simultaneous distillation and extraction process,
402 which gave a 24% extraction yield with *N. oculata* [51], and microwave combined with
403 super-critical CO₂ extraction, which achieved a 30% extraction yield with *N. salina* [52].

404 **4. Conclusion**

405 Wet extraction operations (bead milling combined with centrifugal extraction) achieved
406 a final TAG recovery of 73% using CCE technology with *Nannochloropsis gaditana* cul-
407 tivated in N-depleted media. Physiological variables such as cell fragility, and process
408 operating conditions such as harvesting concentration, were found to affect the whole
409 process. The key variables and their interactions during lipid recovery were determined
410 and optimized by RSM analysis. However, CCE uses around eight times more solvent
411 than CPE. Consequently, **further intensification of the extraction step** is required to
412 combine scalability (*i.e.* the CCE process) with a reduction in solvent consumption and
413 emulsification issues for biodiesel production.

414 **Acknowledgements**

415 VH acknowledges the National Science and Technology Council (CONACyT, Mexico)
416 for his research fellowship. All the authors acknowledge the contributions made by B.
417 Le Gouic, J. Tallec, S. Chollet, L. Herve and M. Cueff

418 Funding: This research did not receive any specific grant from funding agencies in
419 the public, commercial, or not-for-profit sectors.

420 **CRedit authorship contribution statement**

421 **Vladimir Heredia: Conceptualization, Formal analysis, Investigation, Writing - Original Draft. Jeremy Pruvost: Writing - Review & Editing, Supervision. Olivier Gonçalves:**
422 **Writing - Review & Editing. Luc Marchal: Conceptualization, Investigation, Writing -**
423 **Review & Editing, Supervision.**
424

425 **Informed Consent, Human/Animal Rights Statement**

426 No conflicts, informed consent, or human or animal rights are applicable to this study.

427 **References**

- 428 [1] Y. Chisti, Biodiesel from microalgae, *Biotechnology Advances* 25 (2007) 294–306.
- 429 [2] T. A. Beacham, C. Bradley, D. A. White, P. Bond, S. T. Ali, Lipid productivity and cell wall
430 ultrastructure of six strains of *Nannochloropsis*: Implications for biofuel production and downstream
431 processing, *Algal Research* 6 (2014) 64–69.
- 432 [3] X. Ma, J. Liu, B. Liu, T. Chen, B. Yang, F. Chen, Physiological and biochemical changes reveal
433 stress-associated photosynthetic carbon partitioning into triacylglycerol in the oleaginous marine
434 alga *Nannochloropsis oculata*, *Algal Research* 16 (2016) 28–35.
- 435 [4] Y. Ma, Z. Wang, C. Yu, Y. Yin, G. Zhou, Evaluation of the potential of 9 *Nannochloropsis* strains
436 for biodiesel production, *Bioresource Technology* 167 (2014) 503–509.
- 437 [5] D. Bouillaud, V. Heredia, T. Castaing-Cordier, D. Drouin, B. Charrier, O. Gonçalves, J. Farjon,
438 P. Giraudeau, Benchtop flow NMR spectroscopy as an online device for the in vivo monitoring of
439 lipid accumulation in microalgae, *Algal Research* 43 (2019) 101624.
- 440 [6] A. Taleb, J. Pruvost, J. Legrand, H. Marec, B. Le-Gouic, B. Mirabella, B. Legeret, S. Bouvet,
441 G. Peltier, Y. Li-Beisson, S. Taha, H. Takache, Development and validation of a screening proce-
442 dure of microalgae for biodiesel production: Application to the genus of marine microalgae *Nan-*
443 *nochloropsis*, *Bioresource Technology* 177 (2015) 224–232.
- 444 [7] K. J. Flynn, K. Davidson, A. Cunningham, Relations between carbon and nitrogen during growth
445 of *Nannochloropsis oculata* (Droop) Hibberd under continuous illumination, *New Phytologist* 125
446 (1993) 717–722.
- 447 [8] J. Camacho-Rodríguez, A. M. González-Céspedes, M. C. Cerón-García, J. M. Fernández-Sevilla,
448 F. G. Ación-Fernández, E. Molina-Grima, A quantitative study of eicosapentaenoic acid (EPA)
449 production by *Nannochloropsis gaditana* for aquaculture as a function of dilution rate, temperature
450 and average irradiance, *Applied Microbiology and Biotechnology* 98 (2014) 2429–2440.
- 451 [9] E. Angles, P. Jaouen, J. Pruvost, L. Marchal, Wet lipid extraction from the microalga *Nan-*
452 *nochloropsis* sp.: Disruption, physiological effects and solvent screening, *Algal Research* 21 (2017)
453 27–34.
- 454 [10] J. H. Janssen, P. P. Lamers, R. C. de Vos, R. H. Wijffels, M. J. Barbosa, Translocation and de novo
455 synthesis of eicosapentaenoic acid (EPA) during nitrogen starvation in *Nannochloropsis gaditana*,
456 *Algal Research* 37 (2019) 138–144.
- 457 [11] V. Montalescot, T. Rinaldi, R. Touchard, S. Jubeau, M. Frappart, P. Jaouen, P. Bourseau, L. Mar-
458 chal, Optimization of bead milling parameters for the cell disruption of microalgae: Process mod-
459 eling and application to *Porphyridium cruentum* and *Nannochloropsis oculata*, *Bioresource Tech-*
460 *nology* 196 (2015) 339–346.
- 461 [12] M. J. Scholz, T. L. Weiss, R. E. Jinkerson, J. Jing, R. Roth, U. Goodenough, M. C. Posewitz, H. G.
462 Gerken, Ultrastructure and composition of the *Nannochloropsis gaditana* cell wall, *Eukaryotic Cell*
463 13 (2014) 1450–1464.
- 464 [13] X. B. Tan, M. K. Lam, Y. Uemura, J. W. Lim, C. Y. Wong, K. T. Lee, Cultivation of microalgae

- 465 for biodiesel production: A review on upstream and downstream processing, *Chinese Journal of*
466 *Chemical Engineering* 26 (2018) 17–30.
- 467 [14] M. Axelsson, F. Gentili, A single-step method for rapid extraction of total lipids from green
468 microalgae, *PLoS ONE* 9 (2014) 17–20.
- 469 [15] S. A. Scott, M. P. Davey, J. S. Dennis, I. Horst, C. J. Howe, D. J. Lea-Smith, A. G. Smith, Biodiesel
470 from algae: Challenges and prospects, *Current Opinion in Biotechnology* 21 (2010) 277–286.
- 471 [16] R. Halim, R. Harun, M. K. Danquah, P. A. Webley, Microalgal cell disruption for biofuel develop-
472 ment, *Applied Energy* 91 (2012) 116–121.
- 473 [17] H. Taher, S. Al-Zuhair, A. H. Al-Marzouqi, Y. Haik, M. Farid, Effective extraction of microalgae
474 lipids from wet biomass for biodiesel production, *Biomass and Bioenergy* 66 (2014) 159–167.
- 475 [18] T. Dong, E. P. Knoshaug, P. T. Pienkos, L. M. Laurens, Lipid recovery from wet oleaginous
476 microbial biomass for biofuel production: A critical review, *Applied Energy* 177 (2016) 879–895.
- 477 [19] A. K. Lee, D. M. Lewis, P. J. Ashman, Disruption of microalgal cells for the extraction of lipids
478 for biofuels: Processes and specific energy requirements, *Biomass and Bioenergy* 46 (2012) 89–101.
- 479 [20] F. Ghasemi Naghdi, L. M. González González, W. Chan, P. M. Schenk, Progress on lipid extraction
480 from wet algal biomass for biodiesel production, *Microbial Biotechnology* 9 (2016) 718–726.
- 481 [21] R. Halim, B. Gladman, M. K. Danquah, P. A. Webley, Oil extraction from microalgae for biodiesel
482 production, *Bioresource Technology* 102 (2011) 178–185.
- 483 [22] H. M. Amaro, A. C. Guedes, F. X. Malcata, Advances and perspectives in using microalgae to
484 produce biodiesel, *Applied Energy* 88 (2011) 3402–3410.
- 485 [23] J. Y. Lee, C. Yoo, S. Y. Jun, C. Y. Ahn, H. M. Oh, Comparison of several methods for effective
486 lipid extraction from microalgae, *Bioresource Technology* 101 (2010) S75–S77.
- 487 [24] J. Kim, G. Yoo, H. Lee, J. Lim, K. Kim, C. W. Kim, M. S. Park, J. W. Yang, Methods of
488 downstream processing for the production of biodiesel from microalgae, *Biotechnology Advances*
489 31 (2013) 862–876.
- 490 [25] T. R. Zinkoné, I. Gifuni, L. Lavenant, J. Pruvost, L. Marchal, Bead milling disruption kinetics of
491 microalgae: Process modeling, optimization and application to biomolecules recovery from *Chlorella*
492 *sorokiniana*, *Bioresource Technology* 267 (2018) 458–465.
- 493 [26] C. Safi, C. Frances, A. V. Ursu, C. Laroche, C. Pouzet, C. Vaca-Garcia, P. Y. Pontalier, Under-
494 standing the effect of cell disruption methods on the diffusion of *Chlorella vulgaris* proteins and
495 pigments in the aqueous phase, *Algal Research* 8 (2015) 61–68.
- 496 [27] J. Folch, M. Lees, G. Sloane Stanley, A simple method for the isolation and purification of total
497 lipides from animal tissues 55 (1987) 999–1033.
- 498 [28] E. G. Bligh, W. J. Dyer, A Rapid Method Of Total Lipid Extraction And Purification, *Canadian*
499 *Journal of Biochemistry and Physiology* 37 (1959) 911–917.
- 500 [29] P. Li, K. Sakuragi, H. Makino, Extraction techniques in sustainable biofuel production: A concise
501 review, *Fuel Processing Technology* 193 (2019) 295–303.
- 502 [30] P. Watts, Chloroform, Technical Report 58, World Health Organization, Geneva, Switzerland, 2004.
503 URL: <https://www.who.int/ipcs/publications/cicad/en/>.

- 504 [31] D. Reay, C. Ramshaw, A. Harvey (Eds.), *Process Intensification*, Elsevier, 2008. doi:10.1016/
505 B978-0-7506-8941-0.X0001-6.
- 506 [32] B. Seyfang, A. Klein, T. Grützner, *Extraction Centrifuges—Intensified Equipment Facilitating*
507 *Modular and Flexible Plant Concepts*, *ChemEngineering* 3 (2019) 17.
- 508 [33] M. Bojczuk, D. Żyżelewicz, P. Hodurek, *Centrifugal partition chromatography – A review of recent*
509 *applications and some classic references*, *Journal of Separation Science* 40 (2017) 1597–1609.
- 510 [34] K. Schügerl, *Solvent Extraction in Biotechnology*, volume 8, Springer Berlin Heidelberg, Berlin,
511 Heidelberg, 1994. doi:10.1007/978-3-662-03064-6.
- 512 [35] C. Ungureanu, L. Marchal, A. A. Chirvase, A. Foucalt, *Centrifugal partition extraction, a new*
513 *method for direct metabolites recovery from culture broth: Case study of torularhodin recovery*
514 *from Rhodotorula rubra*, *Bioresource Technology* 132 (2013) 406–409.
- 515 [36] J. A. Berges, D. J. Franklin, P. J. Harrison, *Evolution of an artificial seawater medium: Improve-*
516 *ments in enriched seawater, artificial water over the last two decades*, *Journal of Phycology* 37
517 (2001) 1138–1145.
- 518 [37] J. Pruvost, G. Van Vooren, B. Le Gouic, A. Couzinet-Mossion, J. Legrand, *Systematic investiga-*
519 *tion of biomass and lipid productivity by microalgae in photobioreactors for biodiesel application*,
520 *Bioresource Technology* 102 (2011) 150–158.
- 521 [38] B. Moutel, O. Gonçalves, F. Le Grand, M. Long, P. Soudant, J. Legrand, D. Grizeau, J. Pruvost,
522 *Development of a screening procedure for the characterization of Botryococcus braunii strains for*
523 *biofuel application*, *Process Biochemistry* 51 (2016) 1855–1865.
- 524 [39] S. Kim, J. Chen, T. Cheng, A. Gindulyte, J. He, S. He, Q. Li, B. A. Shoemaker, P. A. Thiessen,
525 B. Yu, L. Zaslavsky, J. Zhang, E. E. Bolton, *PubChem 2019 update: improved access to chemical*
526 *data*, *Nucleic Acids Research* 47 (2019) D1102–D1109.
- 527 [40] A.-G. Sicaire, M. A. Vian, A. Filly, Y. Li, A. Bily, F. Chemat, *2-Methyltetrahydrofuran: Main*
528 *Properties, Production Processes, and Application in Extraction of Natural Products*, 2014, pp.
529 253–268. doi:10.1007/978-3-662-43628-8_12.
- 530 [41] L. Marchal, J. Legrand, A. Foucalt, *Mass transport and flow regimes in centrifuga partition*
531 *chromatography*, *AIChE Journal* 48 (2002) 1692–1704.
- 532 [42] L. Marchal, M. Mojaat-Guemir, A. Foucalt, J. Pruvost, *Centrifugal partition extraction of β -*
533 *carotene from Dunaliella salina for efficient and biocompatible recovery of metabolites*, *Bioresource*
534 *Technology* 134 (2013) 396–400.
- 535 [43] M. R. Heath, K. Richardson, T. Kirboe, *Optical assessment of phytoplankton nutrient depletion*,
536 *Journal of Plankton Research* 12 (1990) 381–396.
- 537 [44] M. A. Borowitzka, *The ‘stress’ concept in microalgal biology—homeostasis, acclimation and adap-*
538 *tation*, *Journal of Applied Phycology* 30 (2018) 2815–2825.
- 539 [45] J. T. Stuart, *Taylor-Vortex Flow: A Dynamical System*, *SIAM Review* 28 (1986) 315–342.
- 540 [46] M. Nakase, K. Takeshita, *Numerical and Experimental Study on Oil-water Dispersion in New*
541 *Countercurrent Centrifugal Extractor*, *Procedia Chemistry* 7 (2012) 288–294.
- 542 [47] S. Ebert, L. Grossmann, J. Hinrichs, J. Weiss, *Emulsifying properties of water-soluble proteins*

- 543 extracted from the microalgae: *Chlorella sorokiniana* and *Phaeodactylum tricornutum*, *Food and*
544 *Function* 10 (2019) 754–764.
- 545 [48] H. Jiang, Y. Sheng, T. Ngai, Pickering emulsions: Versatility of colloidal particles and recent
546 applications, *Current Opinion in Colloid & Interface Science* 49 (2020) 1–15.
- 547 [49] E. Ryckeboosch, S. P. C. Bermúdez, R. Termote-Verhalle, C. Bruneel, K. Muylaert, R. Parra-
548 Saldivar, I. Foubert, Influence of extraction solvent system on the extractability of lipid components
549 from the biomass of *Nannochloropsis gaditana*, *Journal of Applied Phycology* 26 (2014) 1501–1510.
- 550 [50] H. Sati, M. Mitra, S. Mishra, P. Baredar, Microalgal lipid extraction strategies for biodiesel pro-
551 duction: A review, *Algal Research* 38 (2019) 101413.
- 552 [51] C. Dejoye Tanzi, M. Abert Vian, F. Chemat, New procedure for extraction of algal lipids from wet
553 biomass: A green clean and scalable process, *Bioresource Technology* 134 (2013) 271–275.
- 554 [52] P. D. Patil, K. P. R. Dandamudi, J. Wang, Q. Deng, S. Deng, Extraction of bio-oils from algae
555 with supercritical carbon dioxide and co-solvents, *Journal of Supercritical Fluids* 135 (2018) 60–68.
- 556 [53] G. E. P. Box, D. W. Behnken, Some New Three Level Designs for the Study of Quantitative
557 Variables, *Technometrics* 2 (1960) 455.
- 558 [54] S. L. Ferreira, R. E. Bruns, H. S. Ferreira, G. D. Matos, J. M. David, G. C. Brandão, E. G. da Silva,
559 L. A. Portugal, P. S. dos Reis, A. S. Souza, W. N. dos Santos, Box-Behnken design: An alternative
560 for the optimization of analytical methods, *Analytica Chimica Acta* 597 (2007) 179–186.

561 **Appendix A. CCE operating parameter optimization: RSM approach**

562 *A.1. Introduction*

563 The Box-Behnken response surface methodology (RSM) was designed [53, 54] to
564 clarify the interaction between operating parameters in the CCE wet extractor. Contrary
565 to the usual factorial RSM (where variables are arranged in an n-dimensional space and
566 all combinations are considered for the experiment setup), the Box-Behnken RSM is
567 arranged as a spherical set of variables, which means that the number of experiment runs
568 is reduced and the extreme interaction vertices are not considered. It is advantageous
569 because certain combinations of factors (in this work and others) could be physically
570 restrictive or expensive to operate.

571 Using this RSM, a response surface is obtained that can be modeled and analyzed
572 using the ANOVA method, which looks for the greatest interaction impacting the re-
573 sponse.

574 *A.2. experiment setup*

575 The Box-Behnken RSM included 15 observation units (OUs) for three independent
576 factors and one response variable: 12 OUs derived from independent variables around 3
577 other OUs as replicates of the central point. Ranges and variables were biomass concen-
578 tration (from bead milling) $X = 2, 5, 10$ g/L and solvent and feed inlets S and $F = 5,$
579 $7.5, 10$ mL/min each. The results of experiments carried out with all the observations
580 units performed are presented in Table A.3.

581 The TFA/TAG extraction efficiency ($\eta_{E,i}$) results from the 15 OUs were processed
582 using Design Expert V11 (Stat-Ease, US). For some analyses, the variables were coded
583 as follows: X as A, S as B and F as C. The software provided random experimental
584 design, statistical analysis and numerical and graphical optimization.

585 *A.3. RSM data analysis*

586 After running the Design Expert software, the data were found to fit well with a
587 quadratic-order model. Fig. A.1 shows that with the experiment extraction efficiency
588 $\eta_{E,i}$, which corresponds with a high biomass concentration, X and S cannot actually
589 be fitted into a model because of the sudden increase (mainly due to the unexpected
590 appearance of emulsion at these values).

Table A.3: Experimental results obtained by the Box-Benhken RSM analysis for the **Total Fatty Acid** ($\eta_{E,TFA}$) and Triacylglycerol ($\eta_{E,TAG}$) extraction efficiencies. OU - observation unit; A, B and C are the coded values for **biomass concentration (X), solvent inlet rate (S) and feed inlet rate (F)** respectively.

O.U.	A : X (g/L)	B : S (mL/min)	C : F (mL/min)	$\eta_{E,TFA}$	$\eta_{E,TAG}$
1	2,0	7,5	10,0	84%	81%
2	2,0	7,5	5,0	55%	48%
3	2,0	5,0	7,5	42%	41%
4	2,0	10,0	7,5	15%	13%
5	5,0	10,0	5,0	73%	62%
6	5,0	7,5	7,5	70%	74%
7	5,0	7,5	7,5	70%	74%
8	5,0	10,0	10,0	44%	30%
9	5,0	5,0	10,0	78%	79%
10	5,0	5,0	5,0	59%	56%
11	5,0	7,5	7,5	70%	73%
12	10,0	10,0	7,5	82%	80%
13	10,0	7,5	10,0	51%	34%
14	10,0	7,5	5,0	60%	52%
15	10,0	5,0	7,5	21%	19%

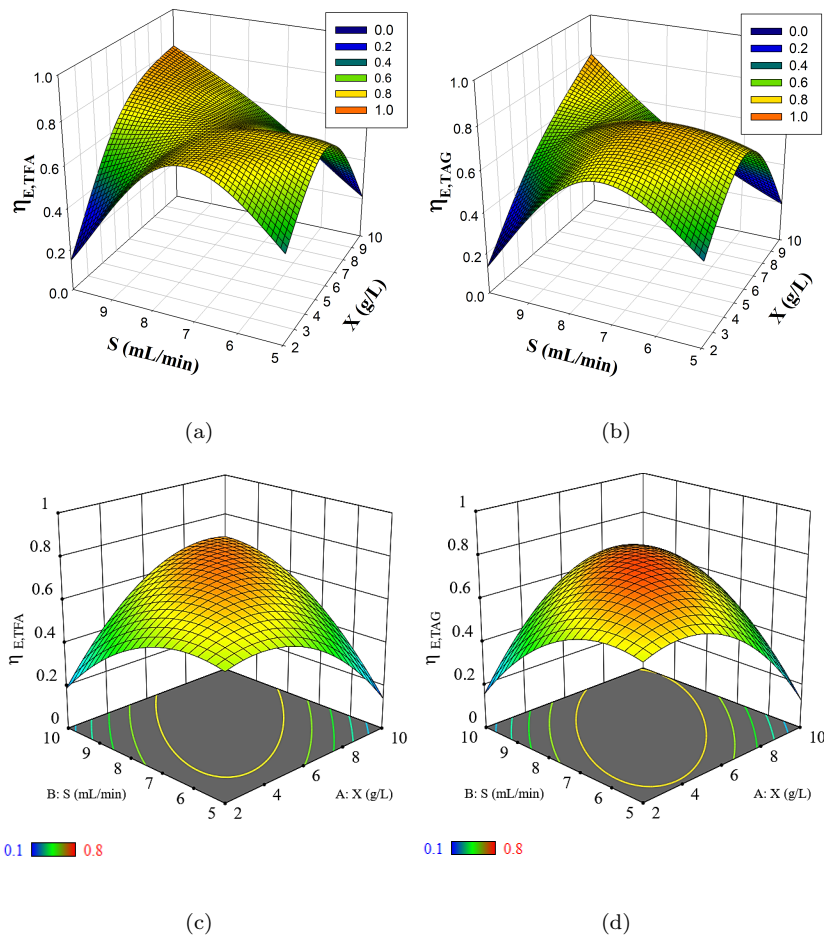


Figure A.1: Raw experiment data and quadratic 3D mesh model for the influence of solvent-to-biomass concentration on extraction efficiency, $\eta_{E,i}$. a) and b) unprocessed data for Total Fatty Acid (TFA) and Triacylglycerol (TAG) respectively. c) and d) data obtained after modeling

Table A.4: Analysis of variance (ANOVA) for modeling of a quadratic order. Values for surface response on **Total Fatty Acid (TFA) and Triacylglycerol (TAG)** extraction efficiency are shown.

Source	AGT					TAG				
	SS	df	Mean Square	F-value	p-value	SS	df	Mean Square	F-value	p-value
<i>Model</i>	0.4980	9	0.0553	2.730	0.141	0.5790	9	0.0643	2.150	0.207
<i>A-Biomass conc.</i>	0.0033	1	0.0033	0.164	0.702	0.0001	1	0.0001	0.003	0.962
<i>B-Solvent</i>	0.0156	1	0.0156	0.770	0.420	0.0026	1	0.0026	0.088	0.779
<i>C-Feed</i>	0.0001	1	0.0001	0.001	0.977	0.0003	1	0.0003	0.010	0.925
<i>AB</i>	0.2179	1	0.2179	10.740	0.022	0.2303	1	0.2303	7.700	0.039
<i>AC</i>	0.0279	1	0.0279	1.380	0.294	0.0557	1	0.0557	1.860	0.231
<i>BC</i>	0.0553	1	0.0553	2.730	0.160	0.0727	1	0.0727	2.430	0.180
<i>A²</i>	0.0892	1	0.0892	4.400	0.090	0.1307	1	0.1307	4.370	0.091
<i>B²</i>	0.0765	1	0.0765	3.770	0.110	0.1006	1	0.1006	3.360	0.126
<i>C²</i>	0.0246	1	0.0246	1.210	0.321	0.0002	1	0.0002	0.007	0.937
<i>Std.Dev.</i>			0.142					0.173		
<i>Mean</i>			0.582					0.546		
<i>C.V.%</i>			24.482					31.700		
<i>R²</i>			0.831					0.795		

591 The analysis of variance (Table A.4) showed that first-order sources (A, B and C)
592 seem to have less significance than second-order sources (AB, AC, BC, A², B² and C²).
593 On the whole, interactions and additives affected the model response more than isolated
594 variables: AB and A² are the only ones below $\alpha = 0.1$. The same trends were obtained
595 for TFA and TAG.

596 The results reported in the section 3.5 for maximum extraction efficiency in the model
597 were obtained using $\alpha = 0.05$ in the numerical solution provided by the Design Expert
598 software.

599 The estimated coefficients are shown in table A.5. These represent the expected
600 shift in response per unit factor value, with the other factors constant. To obtain these
601 coefficients using the Box-Benhken RSM, the source values had to be coded as +1 for
602 the higher levels and -1 for the lower ones. This type of analysis enabled identification of
603 the relative impact of the factors by comparing their coefficients. The equation produced
604 with these coefficients could be used to predict the effects in the response, but only within
605 the coded limits of each source.

606 By ignoring the additive variables, for example, the source AB (Coeff_{TFA}: 0.230,
607 Coeff_{TAG}: 0.236) was shown to have the greatest proportional effect on extraction effi-

Table A.5: Estimated regression coefficients in terms of coded factors and final equation coefficients in terms of actual factors, both obtained from the quadratic model obtained for **Total Fatty Acid (TFA)** and **Triacylglycerol (TAG)** wet-extraction efficiency.

Factor	TFA		TAG	
	Coefficient estimate	Final equation coefficient	Coefficient estimate	Final equation coefficient
<i>Intercept</i>	0.712	-0.792	0.753	-1.973
<i>A- Biomass conc.</i>	0.020	0.0206	0.003	0.0634
<i>B-Solvent</i>	0.045	0.3667	0.018	0.4235
<i>C-Feed</i>	0.002	-0.005	-0.006	0.247
<i>AB</i>	0.230	0.023	0.236	0.0236
<i>AC</i>	-0.082	-0.008	-0.116	-0.012
<i>BC</i>	-0.118	-0.019	-0.135	-0.022
<i>A²</i>	-0.168	-0.011	-0.204	-0.013
<i>B²</i>	-0.144	-0.023	-0.165	-0.026
<i>C²</i>	0.082	0.0131	-0.008	-0.001

608 ciency $\eta_{E,i}$, followed by an inverse-proportional effect on the relationship between S and
609 F (Coeff_{TFA}: -0.118, Coeff_{TAG}: -0.135). This simply means that if more lipids are to be
610 recovered, a higher S should also be used, but the effect is diminished if F is increased
611 in relation to S . A high concentration would require more time and interface contact
612 with the solvent, which can be achieved by reducing the feed rate for CCE. On the other
613 hand, the effect of the additive variables is also highest for A^2 and B^2 . Table A.5 also
614 shows the coefficients for the equation in terms of actual factors. This could be used
615 to predict the extraction efficiency $\eta_{E,i}$ for given levels of each factor. Here, the levels
616 should be specified in the original units for each factor.

617 Nevertheless, neither type of coefficient obtained for regression in this work can be
618 used to accurately predict extraction efficiency $\eta_{E,i}$ precisely, due to the low R^2 and
619 moderate p-value of the model itself. However, R^2 (0.831 for TFA and 0.795 for TAG)
620 indicates only a reasonable correlation between the experimental and predicted values of
621 the response. Despite this, the model still provides important information on the rela-
622 tionship between the parameters, which is clearer when the contour graphs are analyzed.

623 Note that the reason for using Box-Behnken RSM for this work was to determine the
624 general extraction trend as a function of the main operating parameters (such as biomass
625 concentration and solvent and biomass flow rates) and also to determine an operational
626 CCE work-zone.